TELKOMNIKA Telecommunication, Computing, Electronics and Control
Vol. 19, No. 5, October 2021, pp. 1673~1678
ISSN: 1693-6930, accredited First Grade by Kemenristekdikti, Decree No: 21/E/KPT/2018
DOI: 10.12928/TELKOMNIKA.v19i5.17681

Lower and upper bound intercept probability analysis in amplifier-and-forward time switching relaying half-duplex with impact the eavesdropper

Phu Tran Tin[1], Van-Duc Phan[2], Tan N. Nguyen[3], Nguyen Thai Bao[4], Nguyen Ngoc Diem[5], Nguyen Duc Thinh[6], Minh Tran[7]
[1]Faculty of Electronics Technology, Industrial University of Ho Chi Minh City, Ho Chi Minh City, Vietnam
[2]Faculty of Automobile Technology, Van Lang University, Ho Chi Minh City, Vietnam
[3]Wireless Communications Research Group, Faculty of Electrical and Electronics Engineering, Ton Duc Thang University, Ho Chi Minh City, Vietnam
[4,5,6]Faculty of Electrical and Electronics Engineering, Ton Duc Thang University, Ho Chi Minh City, Vietnam
[7]Optoelectronics Research Group, Faculty of Electrical and Electronics Engineering, Ton Duc Thang University, Ho Chi Minh City, Vietnam

Article Info

Article history:

Received Aug 18, 2020
Revised Jul 14, 2021
Accepted Aug 3, 2021

Keywords:

Energy harvesting
Half-duplex
Outage probability
Two-way

ABSTRACT

In this paper, we proposed and investigated the amplifier-and-forward (AF) time switching relaying half-duplex with impact the eavesdropper. In this system model, the source (S) and the destination (D) communicate with each other via a helping of the relay (R) in the presence of the eavesdropper (E). The R harvests energy from the S and uses this energy for information transferring to the D. For deriving the system performance, the lower and upper bound system intercept probability (IP) is proposed and demonstrated. Furthermore, the Monte Carlo simulation is provided to justify the correctness of the mathematical, analytical expression of the lower and upper bound IP. The results show that the analytical and the simulation curves are the same in connection with the primary system parameters.

Corresponding Author:

Van-Duc Phan
Faculty of Automobile Technology
Van Lang University
Ho Chi Minh City, Vietnam
Email: duc.pv@vlu.edu.vn

1. INTRODUCTION

Nowadays, wireless powered communication network (WPCN) is the best solution for overcoming energy harvesting limitations in wireless-powered communication with the considerable demand for energy in energy-constrained wireless networks. Based on the fact that human-made radio frequency (RF) can carry both energy and information, WPCN is considered the leading solution at our time [1]-[6]. There are many researches focused on the WPCN problem in the communication network. Riihonen *et al.* [7], the authors proposed and investigated the outage probability (OP) of the proposed model system and the practical receiver for energy and information transmission and its advantages for the communication network is investigated in [8]. Then [9] presented and demonstrated the practical energy harvesting model for the communication network. Gopala *et al.* [10] studied the continuous energy and power transmission in the cognitive relaying communication network. In another hand, the time switching (TS) and the power splitting (PS) protocols in the different type of the communication network is proposed and studied in [11]-[15].

The main idea of this paper is investigating the amplifier-and-forward (AF) time switching relaying half-duplex with the impact of the eavesdropper. In this system model, the source (S) and the destination (D) communicate with each other via a helping of the relay (R) in the presence of the eavesdropper (E). The R harvests energy from the S and uses this energy for information transferring to the D. For deriving the system performance, the lower and upper bound system intercept probability (IP) is proposed and demonstrated. Furthermore, the Monte Carlo simulation is provided to justify the correctness of the mathematical, analytical expression of the lower and upper bound IP. The results show that the analytical and the simulation curves are the same in connection with the primary system parameters.

2. SYSTEM MODEL

The system model with one destination, one relay, one source, and one eavesdropper is illustrated in Figure 1. The time switching protocol with the energy harvesting (EH) and Information transmission (IT) phases are drawn in Figure 2 [16]-[20]. From figures, the EH and IT can be analyzed by the below sections.

2.1. EH phase

During the first phase, the received signal at the relay can be given by:

$$y_r = h_{SR} x_s + n_r \quad (1)$$

The average transmits power at the relay can be obtained as:

$$P_r = \frac{E_h}{(1-\alpha)T/2} = \frac{2\eta\alpha T P_s |h_{SR}|^2}{(1-\alpha)T} = \kappa P_s |h_{SR}|^2 \quad (2)$$

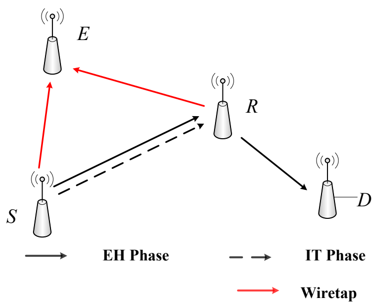

Figure 1. System model

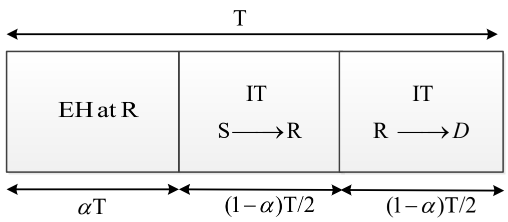

Figure 2. The EH and IT phases

2.2. IT phase

In the second phase, the received signal at the relay can also be given by;

$$y_r = h_{SR} x_s + n_r \quad (3)$$

The received signal at the eavesdropper in the third time slot can be expressed as:

$$y_E^3 = h_{RE} x_r + n_E \quad (4)$$

In this model, we consider amplifier-and-forward (AF) protocol. So, after received the signal from source, relay will amplify that signal by factor β to both destination and eavesdropper as well.

β can be computed as:

$$\beta = \frac{x_r}{y_r} = \sqrt{\frac{P_r}{|h_{sr}|^2 P_s + N_0}} \quad (5)$$

Substituting (5) into (4) and combine with (3), we have:

$$y_E^3 = h_{RE}\beta y_r + n_E = h_{RE}\beta(h_{SR}x_s + n_r) + n_E = \underbrace{h_{RE}h_{SR}x_s\beta}_{signal} + \underbrace{h_{RE}\beta n_r + n_E}_{noise} \quad (6)$$

From (6), the eavesdropper will successfully decode the signal from relay with a given signal to noise ratio (SNR) as following:

$$\gamma_1 = \frac{E\{|signal|^2\}}{E\{|noise|^2\}} = \frac{P_s|h_{SR}|^2|h_{RE}|^2\beta^2}{|h_{RE}|^2\beta^2 N_0 + N_0} \quad (7)$$

After doing some algebra, (7) can be expressed by:

$$\gamma_1 \approx \frac{\kappa\Psi|h_{SR}|^2|h_{RE}|^2}{\kappa|h_{RE}|^2+1} \quad (8)$$

where $\Psi = \frac{P_s}{N_0}$

Next, in the second time slot, the eavesdropper also overhears the information from the source. Hence, the received signal at E can be given as:

$$y_E^2 = h_{SE}x_s + n_E \quad (9)$$

From (9), E can decode the signal from source with the following SNR:

$$\gamma_2 = \Psi|h_{SE}|^2 \quad (10)$$

At the eavesdropper, it will employ the maximal ratio combining (MRC) diversity technical. Therefore, from (8) and (9), the overall SNR at E can be claimed by:

$$\gamma_E = \gamma_1 + \gamma_2 = \frac{\kappa\Psi|h_{SR}|^2|h_{RE}|^2}{\kappa|h_{RE}|^2+1} + \Psi|h_{SE}|^2 \quad (11)$$

3. IP ANALYSIS

3.1. Exact analysis

The IP can be defined by:

$$IP = Pr(\gamma_E > \gamma_{th}) \quad (12)$$

where γ_{th} is the threshold of system. Substituting (11) into (12), the IP can be rewritten as;

$$IP = Pr(X + Y > \gamma_{th}) = 1 - Pr(X + Y \le \gamma_{th}) = 1 - \int_0^{\gamma_{th}} F_X(\gamma_{th} - y|Y = y) \times f_Y(y)dy \quad (13)$$

where $X = \frac{\kappa\Psi|h_{SR}|^2|h_{RE}|^2}{\kappa|h_{RE}|^2+1}, Y = \Psi|h_{SE}|^2$.

Next, the cumulative distribution function (CDF) of X can be computed as;

$$\begin{aligned} F_X(x) &= \Pr\left(\frac{\kappa\Psi|h_{SR}|^2|h_{RE}|^2}{\kappa|h_{RE}|^2+1} < x\right) = \Pr\left(|h_{SR}|^2 < \frac{x}{\Psi} + \frac{x}{\kappa\Psi|h_{RE}|^2}\right) \\ &= \int_0^\infty F_{|h_{SR}|^2}\left(\left[\frac{x}{\Psi} + \frac{x}{\kappa\Psi|h_{RE}|^2}\right] \Big| \, |h_{RE}|^2 = a\right) \times f_{|h_{RE}|^2}(a)da \\ &= 1 - \lambda_{RE}\exp\left(-\frac{x\lambda_{SR}}{\Psi}\right)\int_0^\infty \exp\left(-\frac{x\lambda_{SR}}{\kappa\Psi a}\right) \times \exp(-\lambda_{RE}a)da \end{aligned} \quad (14)$$

And after solve the integral, the CDF in (14) can be reformulated by:

$$F_X(x) = 1 - 2\,exp\left(-\frac{x\lambda_{SR}}{\Psi}\right)\sqrt{\frac{x\lambda_{SR}\lambda_{RE}}{\kappa\Psi}} \times K_1\left(2\sqrt{\frac{x\lambda_{SR}\lambda_{RE}}{\kappa\Psi}}\right) \quad (15)$$

The CDF of Y can be computed as (16);

$$F_Y(y) = Pr(Y < y) = Pr(\Psi|h_{SE}|^2 < y) = Pr\left(|h_{SE}|^2 < \frac{y}{\Psi}\right) = 1 - exp\left(-\frac{y\lambda_{SE}}{\Psi}\right) \quad (16)$$

where λ_{SE} is the mean of RV $|h_{SE}|^2$. From (16), the probability density function (PDF) of Y can be obtained as;

$$f_Y(y) = \frac{\partial F_Y(y)}{\partial y} = \frac{\lambda_{SE}}{\Psi}\exp\left(-\frac{y\lambda_{SE}}{\Psi}\right) \quad (17)$$

Substituting (15) and (17) into (13), we have:

$$IP = 1 - \frac{\lambda_{SE}}{\Psi}\int_0^{\gamma_{th}}\left\{1 - 2\,exp\left(-\frac{(\gamma_{th}-y)\lambda_{SR}}{\Psi}\right)\sqrt{\frac{(\gamma_{th}-y)\lambda_{SR}\lambda_{RE}}{\kappa\Psi}} \times K_1\left(2\sqrt{\frac{(\gamma_{th}-y)\lambda_{SR}\lambda_{RE}}{\kappa\Psi}}\right)\right\} \times exp\left(-\frac{y\lambda_{SE}}{\Psi}\right)dy \quad (18)$$

3.2. Lower and upper bound IP analysis

It is easy to observe that (18) is very difficult to calculate in closed-form. Hence, in this section, we will perform the IP of system in term of lower and upper bound form. We have the following rule:

$$2\min(X,Y) \le X + Y \le 2\max(X,Y) \quad (19)$$

Therefore, the IP of system in lower bound form can be given by:

$$\begin{aligned} IP_{LB} &= \Pr\left[2\min(X,Y) > \gamma_{th}\right] = \Pr\left[\min(X,Y) > \frac{\gamma_{th}}{2}\right] \\ &= \left(1 - \Pr\left[X \le \frac{\gamma_{th}}{2}\right]\right)\left(1 - \Pr\left[Y \le \frac{\gamma_{th}}{2}\right]\right) \\ &= \left(1 - F_X\left[\frac{\gamma_{th}}{2}\right]\right)\left(1 - F_Y\left[\frac{\gamma_{th}}{2}\right]\right) \end{aligned} \quad (20)$$

Applying the results from (15) and (16), (20) can be claimed by (21).

$$IP_{LB} = 2\exp\left(-\frac{\gamma_{th}}{2\Psi}\left[\lambda_{SR} + \lambda_{SE}\right]\right)\sqrt{\frac{\gamma_{th}\lambda_{SR}\lambda_{RE}}{2\kappa\Psi}} \times K_1\left(\sqrt{\frac{2\lambda_{th}\lambda_{SR}\lambda_{RE}}{\kappa\Psi}}\right) \quad (21)$$

Similar as above, the upper bound IP can be expressed as (22):

$$\begin{aligned} IP_{UB} &= \Pr\left[2\max(X,Y) > \gamma_{th}\right] = \Pr\left[\max(X,Y) > \frac{\gamma_{th}}{2}\right] \\ &= 1 - F_X\left(\frac{\gamma_{th}}{2}\right)F_Y\left(\frac{\gamma_{th}}{2}\right) \\ &= 1 - \left\{1 - 2\exp\left(-\frac{\gamma_{th}\lambda_{SR}}{2\Psi}\right)\sqrt{\frac{\gamma_{th}\lambda_{SR}\lambda_{RE}}{2\kappa\Psi}} \times K_1\left(\sqrt{\frac{2\gamma_{th}\lambda_{SR}\lambda_{RE}}{\kappa\Psi}}\right)\right\}\left\{1 - \exp\left(-\frac{\gamma_{th}\lambda_{SE}}{2\Psi}\right)\right\} \end{aligned} \quad (22)$$

4. NUMERICAL RESULTS AND DISCUSSION

The model system's system performance is investigated using the Monte Carlo simulation as in [21]-[25]. The function of the system IP versus ψ for three cases with exact, lower, and upper bond analysis is provided in Figure 3, respectively. In Figure 3, we set the main system parameters as γ_{th}=1, ψ=1 dB, and η=1 in tree cases with exact analysis, upper and lower bond analysis. As drawn in Figure 3, we can see that the system IP of three cases has a massive rise with varying of ψ from -4 to 14 dB. Furthermore, the system IP versus α is illustrated in Figure 4 with the primary system parameters as γ_{th}=1, α=0.85, and η=1. When α increases from 0 to 1, the system IP increases significantly for three cases with exact analysis, upper and lower bond analysis, as drawn in Figure 4. From the results shown in Figures 3 and 4, we can state that the simulation curves are the same as the analytical curves for three cases with exact analysis, upper and lower bond analysis.

Moreover, we investigated the influence of η and ψ_{th} on the system IP, as shown in Figures 5 and 6, respectively. In this investigation, we set γ_{th}=1, ψ=1 dB, and α=0.5 for Figure 5 and α=0.85, ψ=3 dB, and η=1 for Figure 6. Figure 5 shows that the system IP has a rise with increasing η from 0 to 1 and Figure 6 demonstrates that the system IP has a considerable decrease with the rising of γth from 0.5 to 5. In all Figures 5 and 6, the simulation values agree well with the analytical values for demonstrating the mathematical, analytical section.

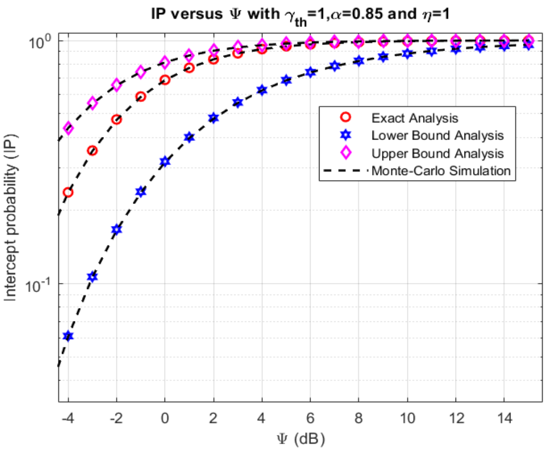

Figure 3. IP versus ψ

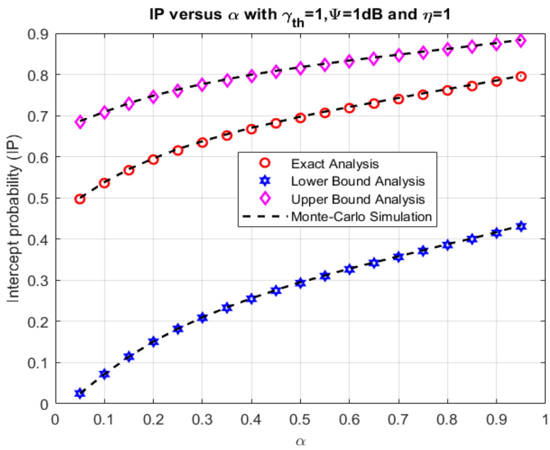

Figure 4. IP versus α

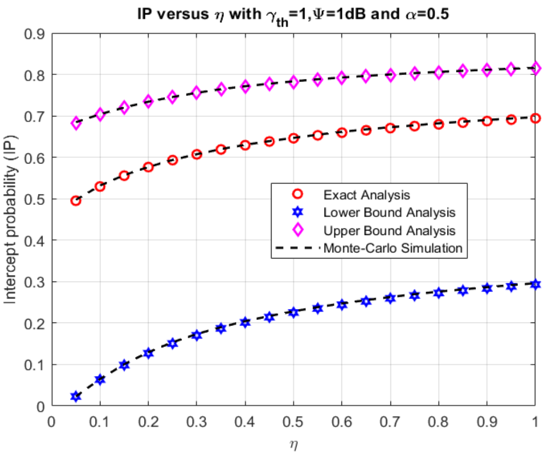

Figure 5. IP versus η

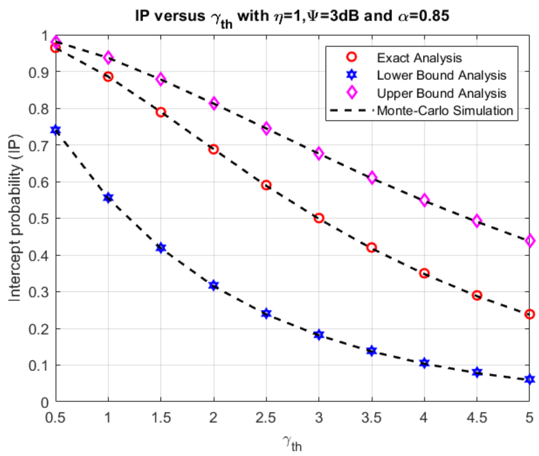

Figure 6. IP versus γ_{th}

5. CONCLUSION

In this paper, the AF time switching relaying half-duplex with impact the eavesdropper is studied. The lower and upper bound system intercept probability (IP) are proposed and demonstrated to derive the system performance. Furthermore, the Monte Carlo simulation is provided to justify the correctness of the mathematical, analytical expression of the lower and upper bound IP. The results show that the analytical and the simulation curves are the same in connection with the primary system parameters.

REFERENCES

[1] S. Bi, C. K. Ho, and R. Zhang, "Wireless powered communication: Opportunities and challenges," *IEEE Commun. Mag*, vol. 53, no. 4, pp. 117-125, 2015, doi: 10.1109/mcom.2015.7081084.

[2] D. Niyato, D. I. Kim, M. Maso, and Z. Han, "Wireless Powered Communication Networks: Research Directions and Technological Approaches," *IEEE Wireless Communications,* vol. 24, no. 6, pp. 2-11, 2017, doi: 10.1109/mwc.2017.1600116.

[3] H. Yu, H. Lee, and H. Jeon, "What is 5G? Emerging 5G Mobile Services and Network Requirements," *Sustainability,* vol. 9, no. 10, pp. 1-22, 2017, doi: 10.3390/su9101848.

[4] X. Zhoun, R. Zhang, and C. K. Ho, "Wireless Information and Power Transfer: Architecture Design and Rate-Energy Tradeoff," *IEEE Trans. Commun*., vol. 61, no. 11, pp. 4754-4767, 2013, doi: 10.1109/tcomm.2013.13.120855.
[5] S. A. G. Shirazi, "Impact of a Time-Varying Rician Fading Channel on the Performance of Alamouti Transmit Diversity Technique," *Conference: 18th IEEE Annual Symposium on Personal Indoor and Mobile Radio Communications (IEEE PIMRC 2007),* Athens, 2007, pp. 1-4, doi: 10.1109/PIMRC.2007.4394407.
[6] T. N. Nguyen, M. Tran, T. L. Nguyen, D. H. Ha, and M. Voznak, "Performance Analysis of a User Selection Protocol in Cooperative Networks with Power Splitting Protocol-Based Energy Harvesting Over Nakagami-m/Rayleigh Channels," *Electronics,* vol. 8, no. 4, 2019, doi: 10.3390/electronics8040448.
[7] Riihonen, Taneli, S. Werner, and R. Wichman, "Hybrid Full-Duplex/Half-Duplex Relaying with Transmit Power Adaptation," *IEEE Transactions on Wireless Communications,* vol. 10, no. 9, pp. 3074-3085, 2011, doi: 10.1109/twc.2011.071411.102266.
[8] T. N. Nguyen *et al.,* "Performance Enhancement for Energy Harvesting Based Two-way Relay Protocols in Wireless Ad-hoc Networks with Partial and Full Relay Selection Methods," *Ad Hoc Networks*, vol. 84, pp. 178-87, 2019, doi: 10.1016/j.adhoc.2018.10.005.
[9] R. Liu, I. Maric, P. Spasojevic, and R. D. Yates, "Discrete Memoryless Interference and Broadcast Channels with Confidential Messages: Secrecy Rate Regions." *IEEE Transactions on Information Theory,* vol. 54, no. 6, pp. 2493-2507, 2008, doi: 10.1109/tit.2008.921879.
[10] P. K. Gopala, L. Lai, and H. El Gamal, "On the Secrecy Capacity of Fading Channels," *IEEE Transactions on Information Theory*, vol. 54, no. 10, pp. 4687-4698, Oct. 2008, doi: 10.1109/TIT.2008.928990
[11] L. Sun and Q. Du, "A Review of Physical Layer Security Techniques for Internet of Things: Challenges and Solutions," *Entropy,* vol. 20, no. 10, 2018, doi: 10.3390/e20100730.
[12] A. Kuhestani, A. Mohammadi, and M. Mohammadi, "Joint Relay Selection and Power Allocation in Large-Scale MIMO Systems with Untrusted Relays and Passive Eavesdroppers," *IEEE Transactions on Information Forensics and Security*, vol. 13, no. 2, pp. 341-355, 2017, doi: 10.1109/tifs.2017.2750102.
[13] L. Hu *et al.,* "Cooperative Jamming for Physical Layer Security Enhancement in Internet of Things," *IEEE Internet of Things Journal,* vol, 5, no. 1, pp. 219-28, 2018, doi: 10.1109/jiot.2017.2778185.
[14] P. T. Tin, D. T. Hung, N. N. Tan, and T. T. Duy, "Secrecy Performance Enhancement for Underlay Cognitive Radio Networks Employing Cooperative Multi-Hop Transmission with and without Presence of Hardware Impairments," *Entropy*, vol. 21, no. 2, 2019, doi: 10.3390/e21020217.
[15] R. Zhao, Y. Yuan, L. Fan, and Y. C. He, "Secrecy Performance Analysis of Cognitive Decode-and-Forward Relay Networks in Nakagami-m Fading Channels," *IEEE Trans. Commun*., vol. 65, no. 2, pp. 549-563, 2017, doi: 10.1109/TCOMM.2016.2618793.
[16] P. T. Tin, P. M. Nam, T. T. Duy, and P. Tran, "Secrecy Performance of TAS/SC-Based Multi-Hop Harvest-to-Transmit Cognitive WSNs Under Joint Constraint of Interference and Hardware Imperfection," *Sensors*, vol. 19, no. 5, pp. 1-20, 2019, doi: 1160. doi:10.3390/s19051160.
[17] T. D. Hieu, T. T. Duy, and B. B. Kim, "Performance Enhancement for Multi-hop Harvest-to-Transmit WSNs with Path-Selection Methods in Presence of Eavesdroppers and Hardware Noises," *IEEE Sensors Journal,* vol. 2, no. 12, pp. 5173-5186, 2018, doi: 10.1109/JSEN.2018.2829145.
[18] T. N. Nguyen, T. H. Q. Minh, P. T. Tran, M. Vozňák, "Performance Analysis of a User Selection Protocol in Cooperative Networks with Power Splitting Protocol-Based Energy Harvesting Over Nakagami-m/Rayleigh Channels," *Electronics,* vol. 8, no. 4, 2019, doi: 10.3390/electronics8040448.
[19] Niyato, Dusit, D. I. Kim, M. Maso, and Z. Han, "Wireless Powered Communication Networks: Research Directions and Technological Approaches." *IEEE Wireless Communications*, pp. 2-11, 2017, doi: 10.1109/mwc.2017.1600116.
[20] Y. Gu, H. Chen, Y. Li, and B. Vucetic, "An adaptive transmission protocol for wireless-powered cooperative communications," In *Proceedings of the IEEE International Conference on Communications (ICC),* London, UK, 8-12 June 2015, pp. 4223-4228.
[21] H. Ju and R. Zhang, "Throughput Maximization in Wireless Powered Communication Networks," *IEEE Trans. Wirel. Commun.,* vol. 13, no. 1, pp. 418-428, 2014, doi: 10.1109/TWC.2013.112513.130760.
[22] M. R. Bhatnagar, "On the Capacity of Decode-and-Forward Relaying over Rician Fading Channels," *IEEE Commun. Lett*., vol. 17, no. 6, pp. 1100-1103, 2013, doi:10.1109/lcomm.2013.050313.122813.
[23] D. Zwillinger and V. Moll, "Table of Integrals, Series, and Products," Springer: NY, USA, 2015. doi: 10.1016/c2010-0-64839-5.
[24] A. A. Nasir, X. Zhou, S. Durrani, and R. A. Kennedy, "Relaying Protocols for Wireless Energy Harvesting and Information Processing," *IEEE Trans. Wirel. Commun*., vol. 12, no. 7, pp. 3622-3636, 2013, doi: 10.1109/twc.2013.062413.122042.
[25] S. Li, C. Li, S. Jin, M. Wei, and L. Yang, "SINR balancing techniques for robust beamforming in V2X-SWIPT system based on a non-linear EH model," *Physical Communications*, vol. 29, no. 8, pp. 95-102, 2018, doi: 10.1016/j.phycom.2018.04.017.